ΣΥΝΕΔΡΙΑ ΤΗΣ 27ΗΣ ΦΕΒΡΟΥΑΡΙΟΥ 1992

ΠΡΟΕΔΡΙΑ ΜΙΧΑΗΛ ΣΑΚΕΛΛΑΡΙΟΥ

ΜΗΧΑΝΙΚΗ.— **Anisotropic thermo-oxidative stability of polymeric composites,** by corresponding member of the Academy *James C. Seferis* and *Jae-Do Nam**.

ABSTRACT

The thermo-oxidative stability of toughened unidirectional bismaleimide/carbon fiber composites produced through a layering process was evaluated in isothermal air aging experiments. By carefully examining different sample size and anisotropic effects with weight loss measurements, degradation rates in the three principal directions were determined, exhibiting different degradation mechanisms in each direction. Effective diffusion coefficients based on a reacted "ash" zone were calculated for three principal directions and utilized to predict the composite degradation rates for various specimens with different fiber orientations and sizes. The developed model equations quantitatively predicted weight loss data, demonstrating the validity of a 3-D anisotropic composite degradation methodology. Finally, the degradation zone was microscopically observed to move into the unreacted «core» zone as aging time increased, and was found to be significantly dependent on the fiber orientation pertaining to the composite anisotropy. Both the theory and experimental results demonstrated conclusively that the thermo-oxidative stability (TOS) of fiber reinforced composites is a tensorial based property (i.e., it depends on magnitude and direction) although it is traditionally measured through scalar weight loss measurements.

INTRODUCTION

High performance polymeric composites have been recognized as attractive engineering materials du to their high strength and light weight. Utilization of high performance polymer composites as structural materials in supersonic

---

* ΔΗΜ. ΣΕΦΕΡΗ, JAE-DO NAM, **Ἀνισότροπος θερμοοξειδικὴ εὐστάθεια ἰνωδῶν συνθέτων ὑλικῶν.**

aircraft place an additional temperature demand ranging from 350°F to 400°F (177°C to 204°C) with several thousand static cycle exposures depending on structural requirements and airplane speed. In addition, high performance polymer composites are increasingly being considered for aircraft engine structural components with use temperatures as high as 700°F (371°C), and eventually up to 780°F (416°C) after periodic exposure to ambient conditions with high humidity [1, 2].

For these more hostile conditions of service temperature and humidity, composite stability characterizations have emerged as an important issue in high temperature composite applications. Weight loss measurements are most often used in assessing composite stability since they are quite simple and accurate, and may be correlated with other physical properties related to degradation/stabilization [3]. However, weight loss measurements of PMR-15 based composites were found to be significantly dependent on sample geometry during isothermal aging in an oxidative environment [1, 4-6]. If the composite weight loss dependence on the sample geometry and its size is not quantitatively identified, the simplicity and accuracy of weight loss measurements cannot be utilized for assessing composite stability. Consequently, consistency in composite weight loss measurements can only be accomplished by careful descriptions of sample characteristics and inherent anisotropy in composite materials.

In this study, an "unreacted core" model, which has been developed for homogeneous isotropic gas-solid reaction systems, was adapted in developing a composite degradation methodology [3]. Two reaction-controlling mechanisms, based on the "unreacted core" model, were reviewed to derive model equations for one-dimensional plane geometry. These models were then extended to describe more complex composite degradation systems pertaining to an anisotropic three-dimensional geometry. Performing isothermal aging experiments with a highly-toughened model Bismaleimide/carbon fiber composite system at 290°C, the extended model was applied to describe the anisotropic and size-dependent weight loss behavior of heterogeneous and anisotropic composite systems. Finally, optical microscopy was utilized to validate the "unreacted core" model assumptions pertaining to specific degradation mechanisms.

THEORETICAL BACKGROUND

When a reaction process is observed to occur first at the outer skin of a solid material, and the reaction zone moves into the solid, the unreacted core model can be utilized to describe the reaction behavior [7, 8]. The reaction process leaves behind some converted material which may be referred to as "ash", and an "unreacted core" of material which shrinks in size during reaction, as shown in Fig. 1. As a starting point, two kinds of possible reaction resistance were considered: diffusion controlled and chemical reaction controlled processes for one-dimensional plane geometry.

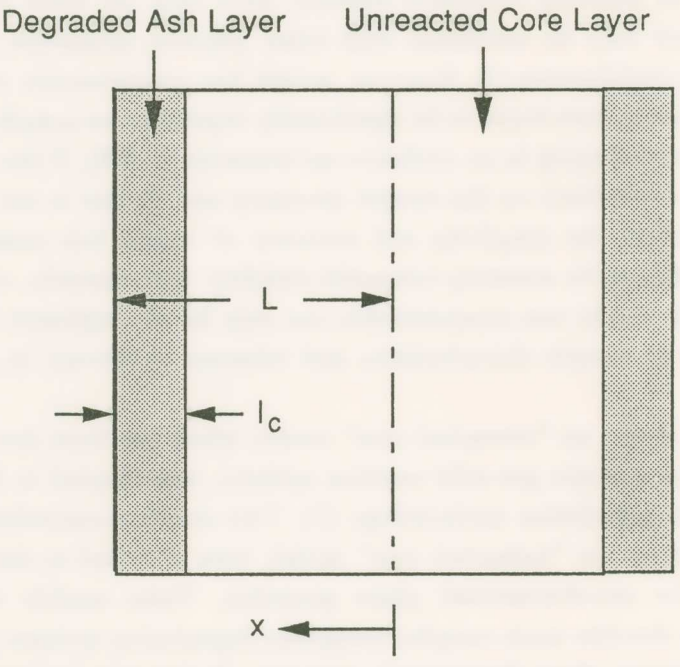

Fig. 1. Schematic representation of composite degradation process based on the unreacted core model.

Diffusion controlled composite degradation

As illustrated in Fig. 1, when the resistance to diffusion through the degraded composite controls the rate of degradation weight loss, both oxygen and the baoundary of the unreacted core move inward toward the center of the composite. In this system, it is generally assumed that the shrinkage of

the unreacted core is slower than the diffusion rate of oxygen toward the unreacted core, which has been considered a reasonable assumption in gas-solid reactions [7, 8]. Then, the reaction rate of oxygen, dN_A/dt, at any instant is given by its rate of diffusion to the reaction surface [7]:

$$-\frac{dN_A}{dt} = A\, q'_A = \text{constant} \tag{1}$$

where N_A is the moles of oxygen, and q'_A is the mole flux of oxygen in the unit of mole cm^{-2} sec^{-1}, and A is the exposed surface area. The oxygen flux within the degraded composite layer may be expressed by Fick's law. Then, noting that both q'_A and dC_A/dx are positive;

$$q'_A = D\frac{dC_A}{dx} \tag{2}$$

where D is effective diffusion coefficient of oxygen in the diffusion layer. Combining eqns (1) and (2), we obtain

$$-\frac{dN_A}{dt} = A D \frac{dC_A}{dx} = \text{constant} \tag{3}$$

Integrating the equation across the degraded layer from L to L-l_c;

$$-\frac{dN_A}{dt}\int_{L}^{L\text{-}lc} dx = AD\int_{C_{As}}^{0} dC_A \tag{4}$$

or

$$-\frac{dN_A}{dt} l_C = A D\, C_{As} \tag{5}$$

where C_{As} is oxygen concentration at the composite surface, and l_c is the degraded thickness as shown in Fig. 1.

Thermo-oxidative stability of composite is usually expressed by the composite weight, which may be interrelated to the moles of oxygen consumed by oxidative degradation reactions. Considering the other half of the composite layer in Fig. 1, the composite weight loss may be related to dN_A by defining a conversion factor β, viz:

$$2\, dN_A = \beta\, dM_c \tag{6}$$

where

$$\beta = \frac{\text{g-moles of consumed A}}{\text{grams of composite weight loss}} \tag{7}$$

and M_c is composite weight.

From the mass balance, the composite in a differential layer, dl_c, can be expressed by the density difference between the reacted and the unreacted solid, viz:

$$dM_c = 2A(\rho_d - \rho_o)\, dl_c \tag{8}$$

where ρ_o and ρ_d are the reacted and unreacted composite densities, respectively. Substituting eqns (6) and (8) into (5), we have

$$\beta(\rho_o - \rho_d) l_c \frac{dl_c}{dt} = D C_{As} \tag{9}$$

Integrating the above equation with respect to l_c and t, the amount of composite degradation is expressed as a function of time, viz:

$$l_c^2 = \frac{2D C_{As}}{\beta(\rho_o - \rho_d)} t \tag{10}$$

Consequently, the composite weight loss may be simply expressed by l_c, which increases with time according to the diffusion controlled degradation process. Several forms of weight loss expression have been utilized in the literature defined by initial composite weight (M_o) and transient composite weight (M): normalized weight (M/M_o), extent of weight loss ($\alpha = 1 - M/M_o$), total weight loss ($Q_c = M_o - M = \alpha M_o$). These expressions can be easily converted to one another with a constant initial weight ($M_o = AL\rho_o$). In this study, total weight loss (or total weight loss per unit surface area) was adopted:

$$q_c = Q_c/A = (M_O - M)/A = 2(\rho_o - \rho_d) l_C \tag{11}$$

where M_{co} and M_c are composite weight before and after aging, respectively. $Q_c(q_c)$ is total composite weight loss (per unit surface area).

Substituting eqn (10) into eqn (11), the composite weight loss can be expressed as a function of sample geometry and time, viz:

$$q_c = \frac{Q_c}{A} = D' t^{0.5} \tag{12}$$

where

$$D' = [\, 8(\rho_o - \rho_d) C_{As} D/\beta \,]^{0.5}$$

Consequently, for a diffusion controlled mechanism, weight loss is derived proportional to $t^{0.5}$. In addition, the characteristic dimension of the specimen was found as an exposed surface area for the total composite weight loss.

Chemical reaction controlled degradation process

For the chemical-reaction controlled degradation, the reaction progress is not affected by the presence of the degraded composite layer, but is affected by the reaction kinetics and the available surface area. Based on a first-order reaction assumption, the reaction rate of oxygen at any instant may be given as [7];

$$-\frac{dN_A}{dt} = A\, k_s\, C_{As} = \text{constant} \tag{13}$$

where k_s is first-order rate constant for the surface reaction.

Substituting eqns (6) and (8) into (13), and integrating the resulting equation with respect to l_c and t, the degraded layer thickness, l_c, can be expressed as a function of time:

$$l_c = \left[\frac{k_s\, C_{As}}{\beta\, (\rho_o - \rho_d)}\right] t \tag{14}$$

Finally, eqns (11) and (14) provide the composite weight loss as a function of time for the chemical-reaction controlled degradation process, viz:

$$q_c = Q_c / A = K' t \tag{15}$$

where

$$K' = 2\, k_s\, C_{As} / \beta$$

As with the diffusion-controlled degradation model, the total weight loss of composite is derived to depend on the characteristic sample surface area. Furthermore, the weight loss is derived proportional to t, which is distinguished from the diffusion-controlled degradation model, where weight loss is proportional to $t^{0.5}$.

1-D Model extension for anisotropic composite system

Comparing diffusion controlled and kinetic controlled reaction mechanisms in eqns (12) and (15), the extent of weight loss of anisotropic composites may be expressed by different time exponents as

$$q_c = \frac{Q_c}{A} D_E \, t^n \tag{16}$$

or

$$\alpha_c = \alpha \, M_o = \frac{1}{L} D_e \, t^n \tag{17}$$

where D_E or D_e are constants corresponding either to effective diffusion or kinetic constant as defined by eqn (12) and (15). For n=0.5, the reaction mechanism is likely subject to a diffusion controlled process. If n=1.0, the kinetic controlled process may be dominant. When n is comparable to neither 0.5 nor 1.0, the reaction mechanism will be ascribed to a mixed degradation process, which might be affected by physico-chemical-topological factors of specific fiber reinforced composite systems.

3-D Extended model development

According to the unreacted shrinking core model system, where the reactions occur within a thin surface layer of the specimen, the total weight loss of anisotropic composite material in the principal directions may be expressed as

$$Q_c = \sum_i Q_{c,i} \tag{18}$$

$$= \sum_i A_i \, q_{c,i} \tag{19}$$

$$= \sum_i A_i D_{E,i} \, t^{ni} \tag{20}$$

where i indicates ξ, η, ζ, and D_E is already defined by eqns (16) and (17).

Utilizing eqn (19) for more than three samples with different A_i's, the weight loss per unit surface area in three directions ($q_{c,i}$) can be calculated. Particularly, if the material principal axes coincide with (x, y, z) axes, the composite weight loss in the principal directions (q_ξ, q_η, q_ζ) can be obtained in the form of eqn (20) providing the time exponents n_i in the principal axes.

EXPERIMENTAL

An aging experiment was performed at 290°C in air for the model layered BMI/IM7 composite [9]. The resin content and density of a unidirectional composite (26 plies) were 36.4 wt%, and 1.56 g/cc, respectively. The manufactured composites were postcured at 215°C (420°F).

Fig. 2 schematically represents the sample dimension and fiber orientation, which were carefully prepared to investigate the anisotropic sample characteristics. For convenience, x, y, and z directions are fixed to represent the directions in the width, length, and through-thickness of the samples, respectively. As shown in Table 1, fiber orientation was designed to represent 90°, 75°, 50°, 40°, 15°, and 0° between fiber and exposed surface. The composite surface, denoted by surface A_z in Fig. 2(a) and Table 1, was manufactured in two different forms for each side: a smooth surface that contacted a metal plate, and a rough surface that contacted a bagging cloth during lamination processing. These two surfaces were not polished in sample preparation, and analyzed as an identical surface by taking the average of the two. The other surfaces, A_x and A_y, were polished by a medium-grade sand paper. The composite surface area was designed to vary from 0.18 to 8.0 cm^2 (1 to 44 ratio) in order to emphasize the effect of each surface characteristic on composite weight loss.

Aging experiments were performed using a tube furnace (Lindberg) with 3″ inside diameter, where the air flow rate was fixed at 100 ml/min. The samples were cooled down to 60°C at 5°C/min, and taken out of the furnace to measure the weight immediately. The measured samples were always heated at 5°C/min to 290°C in the tube furnace for the continuing aging experiments.

For optical microscope investigation, aged samples were cut and polished to observe the degraded area as a function of aging time and fiber orientation. Specifically, for composite degradation in the ξ direction (along the fiber direction), A_x surface of the specimen was cut by 45° angle and polished in order to see the degraded composite layer more clearly through the microscope. Therefore, for samples cut by 45° angle, it should be noted that the observed dagradation zone is $1/\sqrt{2}$ times thinner than the observed thickness.

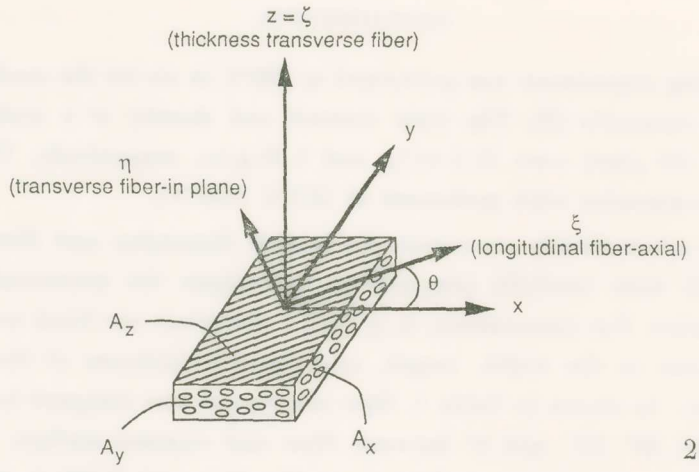

2 (a)

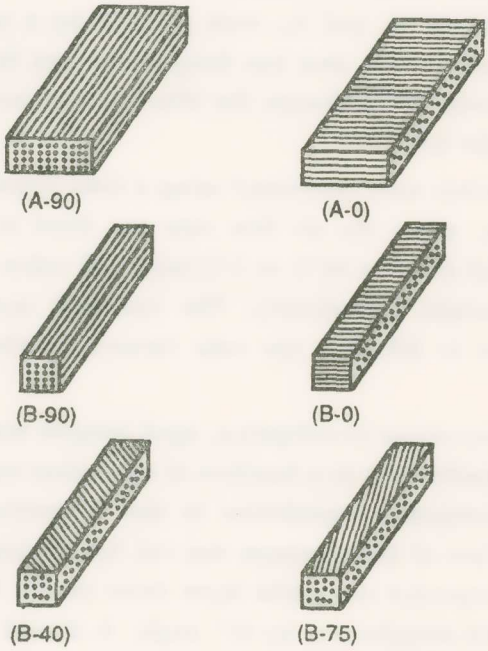

2 (b)

Fig. 2. Sample geometry for aging experiments. Principal axes (ξ, η, ζ) are defined by fiber orientation and (x, y, z) represent directions to the composite width, length, and thickness, respectively.

Table 1. Model layered BMI/IM7 composite samples for 290°C aging experiments.

Sample	weight (gram)	angle (degree)	Ax (cm^2)	Ay (cm^2)	Aza (cm^2)
A-90	4.7222	90	0.756	1.510	0.022
A-0	4.7927	0	1.532	0.768	8.024
B-90	1.2288	90	0.197	1.569	2.007
B-0	1.1868	0	1.522	0.190	2.001
B-40	1.1729	40	1.501	0.188	2.006
B-75	1.1712	75	1.490	0.182	2.001

a Manufactured surface

RESULTS AND DISCUSSION

Anisotropic composite degradation analysis

Figure 3 shows composite weight divided by the original sample weight (M/M_0) as a function of aging time, illustrating a strong geometry dependence of composite degradation. Comparing samples A-90 and B-0, for example, the composite weight loss difference is quite significant. Sample A-90 shows

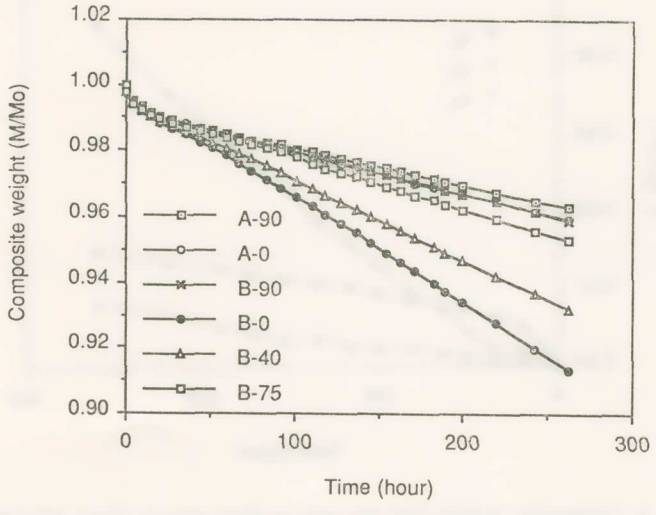

Fig. 3. Composite weight loss data for samples aged at 290°C in air. Denoted sample dimensions are defined in Table 1.

only 3.5% weight loss, but 8.5% weight loss is observed for sample B-0 after 262 hours at 290°C. This geometry-dependent discrepancy appears to become more severe with aging time. It is also interesting to note that there is an inflection point in the weight loss curves in the range of 1-2% of weight loss for all the samples. The composite weight loss rate decelerates up to 1-2% of weight loss, but after this inflection point, it finally shows a seemingly constant weight loss rate. Also, the inflection points seem to depend on the relative magnitude of each surface area pertaining to specific surface characteristics. This behavior was overlooked without detailed analysis in composite weight loss studies because the 1-2% of weight loss could be coupled with the weight loss of absorbed water and/or unreacted monomers. However, this changing weight loss mechanism of composite degradation may be an important composite characteristic, resulting from composite anisotropy and sample size.

In this study, samples A-90, A-0, B-90, and B-0 were first analyzed to obtain $q_{c\xi}$, $q_{c\eta}$, and $q_{c\zeta}$ [g/cm^2], which represents the composite weight loss per unit surface area in the three principal directions. The linear least square method was applied to eqn (19) to calculate q_{ci} in the principal directions for these four samples [14]. The obtained q_{ci}'s are shown in Fig. 4 as a function

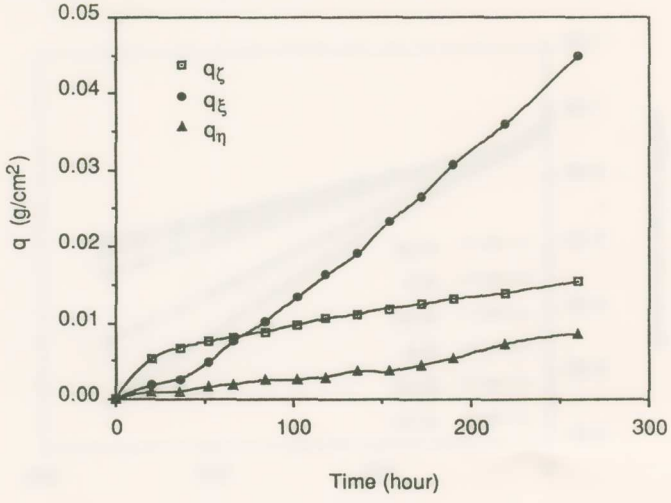

Fig. 4. Composite weight loss per unit surface area in three principal directions. $q_{c\xi}$, $q_{c\eta}$, and $q_{c\zeta}$ denote the axial-to-fiber, transverse-to-fiber, and throught-thickness directions, respectively.

of aging time. $q_{c\zeta}$ represents the composite weight loss in the composite thickness direction, which has a resin-rich layer on the top and bottom surfaces that came during manufacturing in contact with a metal plate and bagging cloth. Furthermore, $q_{c\xi}$ represents the composite weught loss in the axial fiber direction where circular fiber cross sections are exposed to the environment. Finally, $q_{c\eta}$ represents the composite weight loss in the transverse fiber direction, where the fibers are aligned parallel to the exposed surface.

As can be seen in Fig. 4, the composite weight loss in the thickness direction ($q_{c\zeta}$) is dominant before 50 hours of aging. This fast weight loss is likely due to the degradation of resin-rich layer on the exposed surfaces. During this period of time, $q_{c\xi}$ is smaller than $q_{c\zeta}$, but it increases to exceed $q_{c\zeta}$ after 75 hours of aging. After 100 hours of aging, $q_{c\xi}$ becomes quite dominant over $q_{c\zeta}$ and $q_{c\eta}$. It can also be observed that $q_{c\eta}$ is quite small for a period of time, but finally increases to be somewhat comparable to $q_{c\zeta}$. As a result of these findings, the inflection points observed in Fig. 3 may be interpreted as a characteristic feature of the anisotropic composite degradation process. Before the inflection point of 1-2% of weight loss, $q_{c\zeta}$ is dominant in the composite degradation process due to the resin-rich layers on the surfaces, resulting in a fast and decelerating-rate shape in the composite weight loss in Fig. 3. However, when $q_{c\xi}$ exceeds $q_{c\zeta}$ and becomes dominant, the weight loss behavior is likely to follow the shape of $q_{c\xi}$ showing a seemingly constant weight-loss rate.

In order to dermine the time exponents in eqn (16), the obtained values of composite weight loss in the principal directions were plotted as a function of time on a log-log scale as shown in Fig. 5. From the slope and intercept, the following equations were obtained:

$$q_{c\xi} = 10^{-4.508}\, t^{1.31} \tag{21}$$

$$q_{c\eta} = 10^{-4.639}\, t^{1.04} \tag{22}$$

$$q_{c\zeta} = 10^{-2.955}\, t^{0.47} \tag{23}$$

The time exponent of $q_{c\zeta}$, 0.47, compares favorably to the time exponent, 0.5, which was derived from the diffusion-controlled reaction mechanism, eqn (12). In addition, 1.04 for $q_{c\eta}$ is close to 1.0, which was derived from the kinetic-controlled reaction mechanism, eqn (15). However, $q_{c\xi}$ seems to be

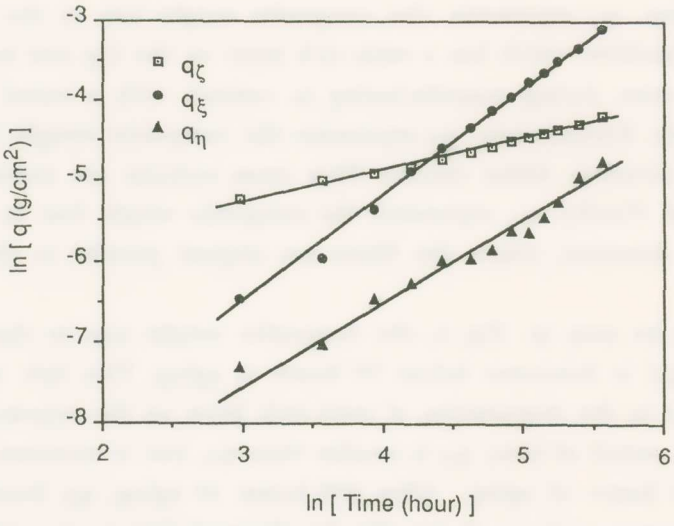

Fig. 5. Composite weight loss per unit surface area in three principal directions ($q_{c\xi}$, $q_{c\eta}$, and $q_{c\zeta}$) plotted in a logarithmic scale.

attributed to none of these, and may be interpreted as a mixed degradation mechanism.

According to these findings, specimen B-40 and B-75 could be analyzed by tensorial transformation of integrated fluxes from the material principal axes to arbitrary x, y, z axes by assuming that the time integral of the fluxes, which is vector, gives a second order tensor. Then, the integrated fluxes in the arbitary directions (q_{cx} and q_{cy}) can be expressed as

$$q_x = q_{c\xi} \cos^2\theta + q_{c\eta} \sin^2\theta \tag{24}$$

$$q_y = q_{c\xi} \sin^2\theta + q_{c\eta} \cos^2\theta \tag{26}$$

$$q_z = q_{c\zeta} \tag{26}$$

Finally, these model equations were utilized to predict the composite weight loss of our model composite system. Fig. 6 compares the experimental data and the model prediction for the specimen with θ=0 or 90 (sample A90, A0, B-90, and B0). As can be seen, they are in good agreement. It is clear that the obtained $q_{c,i}$'s in the principal axes can predict the weight loss of composites with different size and exposed surface area. In addition, the weight-loss inflection points (1-2% of composite weight loss) were accurately described by the model equations, exhibiting the transition from $q_{c\zeta}$ to $q_{c\xi}$ dominance in overall weight loss behavior.

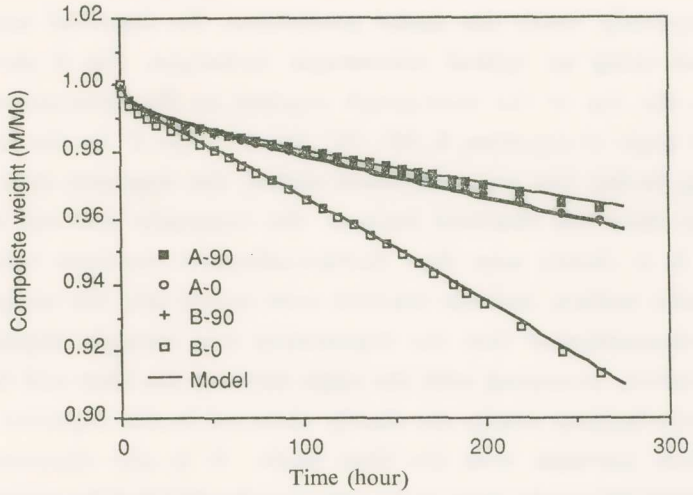

Fig. 6. Composite weight loss data compared with model prediction for the samples with principal axes normal to the exposed surfaces (A90, A0, B90, and B0). Sample dimensions are defined in Table 1.

Figure 7 shows composite weight loss predicted by the developed model for the same size specimen with different orientation (B-90, B-75, B-40, and B-0) exhibiting good agreement between experimental and model results. It is demonstrated that the composite anisotropy strongly affects TOS assessment and that the tensorial treatment of anisotropic diffusion coefficients is required to have a consistent weight loss measurement for its evaluation.

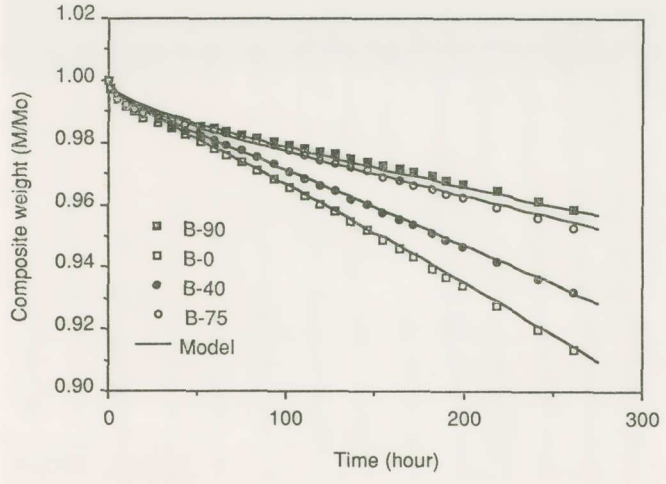

Fig. 7. Composite weight loss data compared with model prediction for samples made with different fiber angles (B90, B75, B40, B0). Sample dimensions are defined in Table 1.

To physically verify the model predictions, the degraded samples were investigated using an optical microscopic technique. Fig. 8 shows an A_x surface on the top of the micrograph exposed to the environment for 164 hours: The angle of exposure, θ, 90°, 75°, 50°, 15°, and 0° for the micrographs shown (Fig. 8a-8e). [As was mentioned earlier, the degraded zone at θ=0 is $1/\sqrt{2}$ times than the observed because the composite was cut at 45° and polished]. It is clearly seen that thermo-odixative reactions take place at the composite surface, and the reaction zone moves into the composite core. It is also demonstrated that the degradation rate strongly depends on the fiber orientation, increasing with the angle between the fiber and the exposed surface. Intra-laminar cracks are clearly observed in the degraded composite region, which increases with the fiber angle. It is also observed that the matrix around the cracks seem to be aggressively attacked by oxygen. Oxygen transport to the composite core region is likely to be enhanced by the intra-laminar cracks, resulting in severe oxidative degradation around the cracks. In addition, the intra-laminar cracks may provide a larger effective surface area for oxidative degradation reactions. As addressed in the model assumption, degradation reactions do not appear to occur along the sharp interface between the composite ash and core.

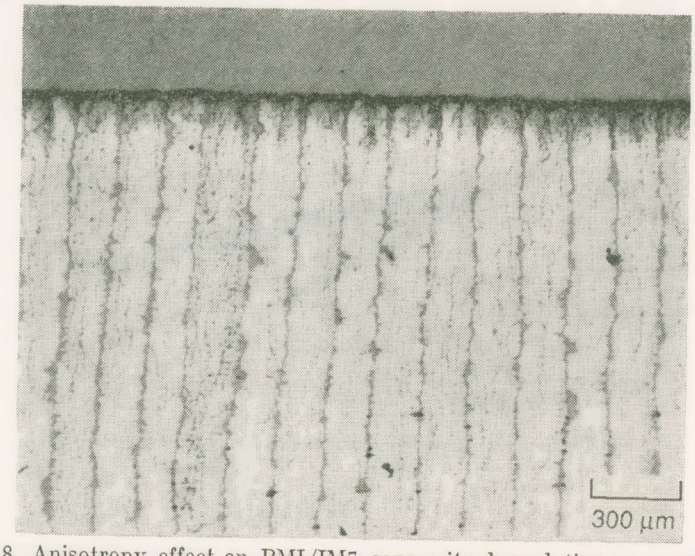

8(a)

Fig. 8. Anisotropy effect on BMI/IM7 composite degradation process aged at 290°C in air for 164 hours. Exposed A_x surface on the top of the micrographs with fiber angle θ: (a) 90°, (b) 75°, (c) 50°, (d) 15°, and (e) 0°.

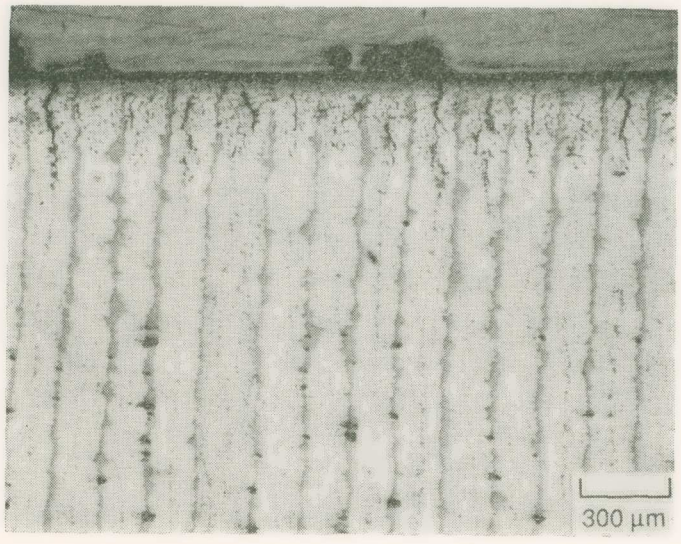

8(b)

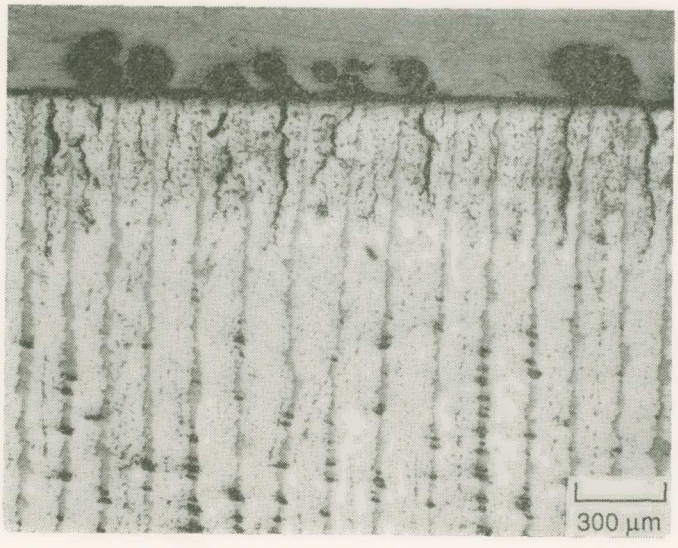

8(c)

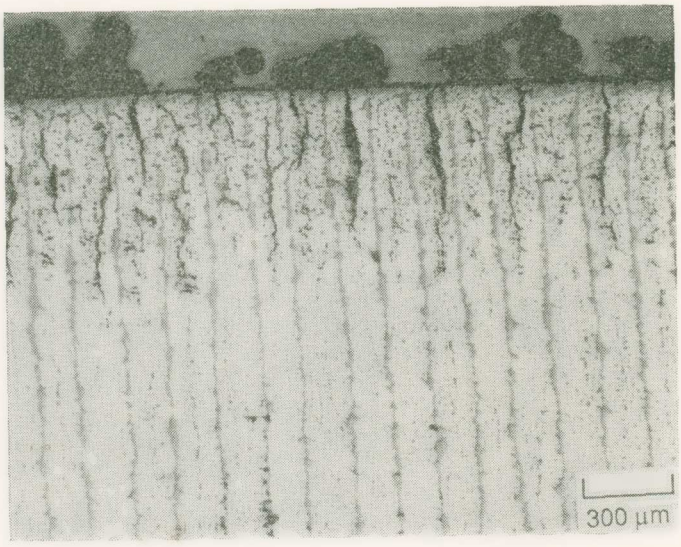

8 (d)

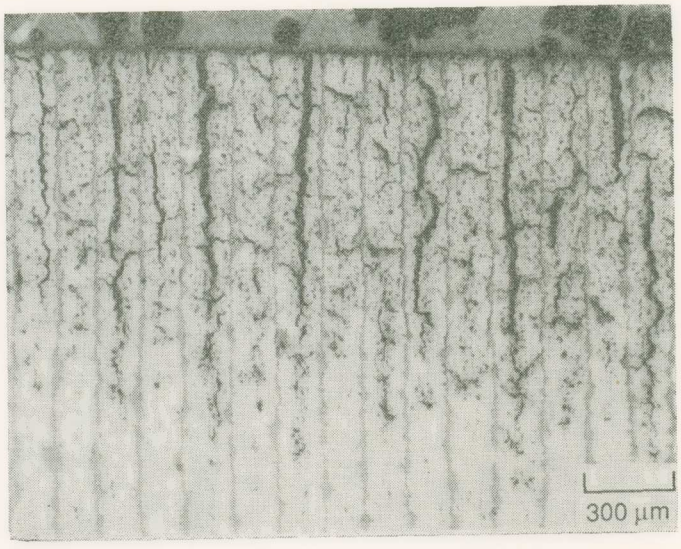

8 (e)

The degradation moving front is shown in Fig. 9 for A_X surface with $\theta=0°$ (i.e., the moving front in the ξ principal direction) after 28, 70, and 262 hour aging, which can also be compared with Fig. 8 (e) for 164 hour aging. Clearly, the degradation zone moves into the composite core with increasing aging time, validating the unreacted core model assumptions. As time passes, the intra-laminar cracks seem to increase in their width and length, and move toward the unreacted core through the fiber axial direction. The degradation moving front in the fiber axial direction seems to be closely related to crack propagation.

Due to degradation reactions resulting in a significant composite weight loss within a thin "ash" layer, the degraded edge of the composite specimen was observed to shrink in the thickness direction. The dimensional mismatch at the interface between the "ash" and "unreacted core" may create an out-of-plane tension especially concentrated at the interface. Intralaminar cracks seem to progress due to this mode I type tension at the ash-core interface as the moving degradation front progresses toward the composite core. Conclusively, the composite degradation rate in the ξ principal direction dominated over the other two degradation rates (see Fig. 4), seemingly because of crack development that resulted in an enhanced oxygen transport and increased reaction surface area. Accordingly, the time exponent of $q_{c\xi}$, which was attributed to neither diffusion- nor kinetic-controlled reaction mechanisms, might be considered as a crack-induced degradation mechanism affecting oxygen transport and effective reaction surface area.

The intra-laminar cracks are not so noticeable for degradation processes in the other principal directions of η and ζ. Fig. 10 shows the manufactured surface on the top of the micrograph compared with the 50°-surface on the side. As can be seen, the manufactured surfaces are not likely to be damaged by the crack-induced oxidation process after 164 hour aging. Manufactured surfaces seem to have the most desirable surface characteristics to be exposed to hostile environmental conditions in terms of weight loss and physical damage in composite degradation processes.

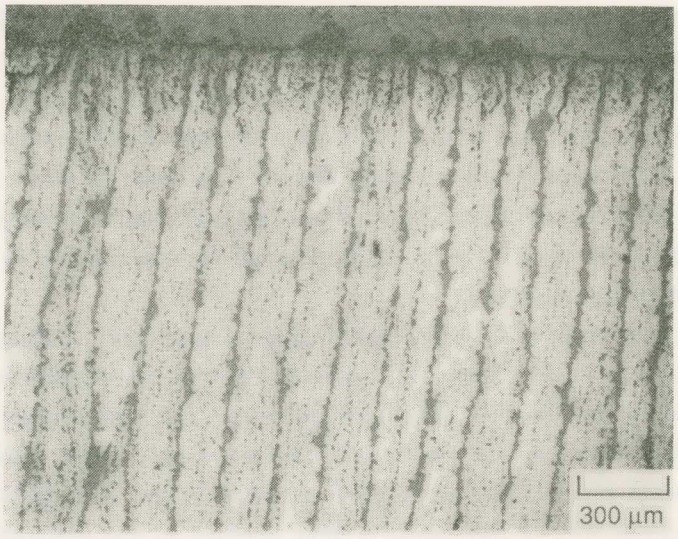

9 (a)

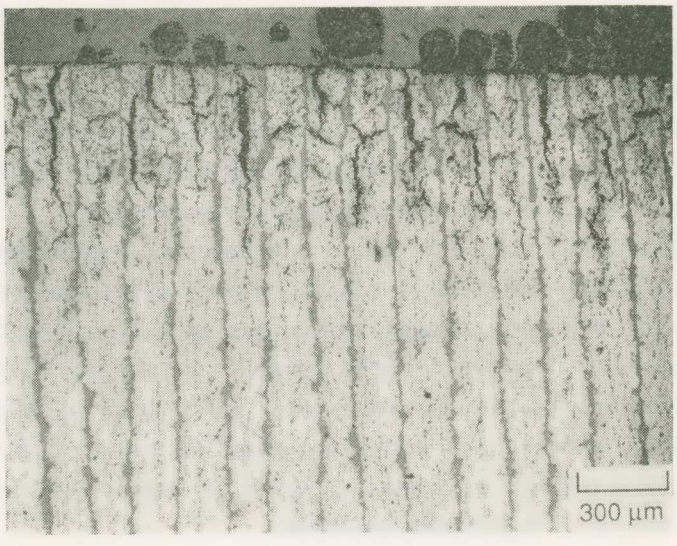

9 (b)

Fig. 9. BMI/IM7 composite degradation zone moving into the core in the ξ-principal direction for 290°C aging. Aging time is (a) 28, (b) 70 and (c) 262 hours. Fig. 8 (e) for 164 hours of aging also provide additional aging data for this sample.

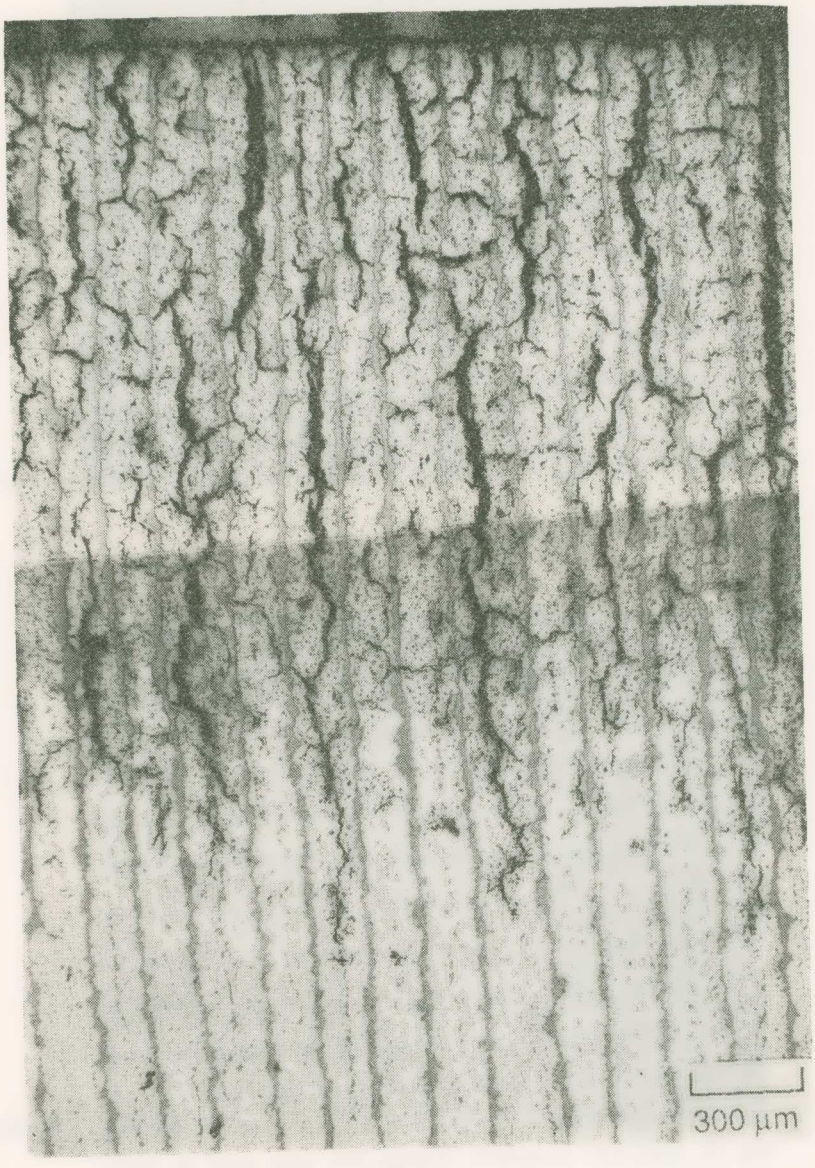

9 (c)

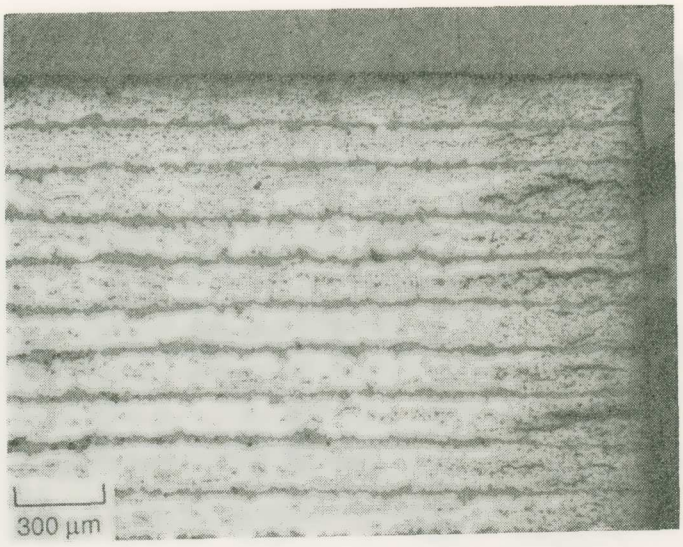

10 (a)

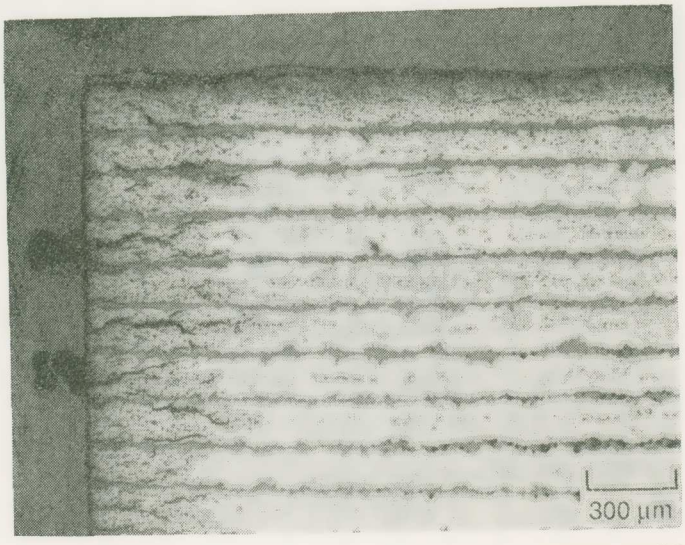

10 (b)

Fig. 10. BMI/IM7 composite degradation zone aged at 290° C for 164 hours (a) manufactured tool-surface and (b) manufactured bagging-surface on the top, for samples with 40° fiber angle to exposed surfaces.

CONCLUSION

Model BMI/graphite fiber composites were investigated as a model composite system for the evaluation of thermo-oxidative stability by isothermal aging experiments at 290°C in an air environment. Aging experiments were carefully designed to identify composite size and anisotropy effects on composite weight loss measurements. Based on theoretical and experimental considerations, a degradation methodology was developed for 3-D anisotropic composite systems.

Correlating the derived model equations and experimental results, anisotropic composite degradation rates in the three principal directions were determined, showing different degradation mechanisms in each direction. Comparing the theoretical and experimental time-exponents of composite degradation rates, composite degradation in the thickness direction ($q_{c\zeta}$) might be ascribed to a diffusion-controlled degradation process. Furthermore, composite degradation in the direction transverse to the fibers ($q_{c\eta}$) was likely controlled by the chemical reaction kinetics. Finally, the crack-induced oxidative degradation was found significant in the direction axial to the fibers ($q_{c\xi}$), which was ascribed neither to diffusion nor reaction controlled degradation mechanism.

Based on these findings, second order tensor components of diffusion coefficient were calculated and utilized to predict the composite degradation rates of the specimens with different fiber angles and sizes. The model equation quantitatively predicted the experimental data with good agreement, demonstrating the validity of the 3-D anisotropic composite degradation methodology.

Furthermore, with a microscopic technique, the degraded zone was clearly observed to move into the unreacted core with increasing aging time validating the model assumptions. The degradation zone was found to be significantly dependent on the fiber orientation pertaining to the composite anisotropy. It was also observed that the resin-rich layer in the model composite system remained more stable than the matrix in the fiber-matrix interphase with respect to the thermo-oxidative degradation. Finally, comparing the three principal axes, the composite degradation in the thickness direction underwent a crack-free degradation process, resulting in desirable surface charactaristics to be exposed to hostile environmental conditions. Collectively, this work establishes, for the first time, a quantitative anisotropic degradation methodology for high performance composites.

ACKNOWLEDGMENTS

The authors express their appreciation to the Boeing Co., B. F. Goodrich, and E. I. du Pont de Nemours & Co., Inc. for their continued support to the Polymeric Composites Laboratory at the University of Washington for developing a fundamental understanding of degradation in polymers and composites.

REFERENCES

1. K. J. Bowles, SQMPE Quarterly, July, 6 (1990).
2. D. A. Scola and J. H. Vontell, Polym. Eng. Sci., 31 (1), 6 (1991).
3. J. - D. Nam, Polymer Matrix Degradation: Characterization and Manufacturing Process for High Temperature Composites, Ph. D. Thesis, Department of Chemical Engineering, University of Washington (1991).
4. F. J. Magendie, Thermal Stability of Ceramic and Carbon Fiber-Reinforced Bismaleimide Matrix Composites, Master's Thesis, Department of Chemical Engineering, University of Washington, Seattle (1990).
5. K. J. Bowles and A. Meyers, 31st International SAMPE Symposium and Exhibition, 1285 (1986).
6. K. J. Bowles and G. Nowak, J. Comp. Mat., 22, 966 (1988).
7. O. Levenspiel, *Chemical Reaction Engineering*, John Wiley & Sons, New York (1972).
8. G. F. Fromet and K. B. Bishoff, Chemical Reactor Analysis and Design, John Wiley & Sons, New York (1979).
9. M. A. Hoisington and J. C. Seferis, American Society for Composites, October, 53 (1991).
10. G. S. G. Beveridge and R. S. Schechter, Optimization: Theory and Practice, McGraw-Hill, Inc., London (1970).

ΠΕΡΙΛΗΨΗ

Ἀνισότροπος εὐστάθεια ἰνωδῶν συνθέτων ὑλικῶν

Σύνθετα ὑλικὰ ὑψηλῆς ἀντοχῆς ἐκ πολυμερῶν οὐσιῶν χρησιμοποιοῦνται εὐρέως ὡς φορτιζόμενα ὑλικὰ εἰς τὰς ἀεροπορικὰς κατασκευὰς διότι παρουσιάζουν ὑψηλὴν εἰδικὴν ἀντοχὴν εἰς φορτίσεις καὶ εἰς δυσκαμψίαν. Ἡ χρησιμοποίησις τῶν συνθέτων αὐτῶν ὑλικῶν ὑψηλῆς ἀντοχῆς εἰς φερούσας κατασκευὰς ὑπερηχητικῶν ἀεροπλάνων

δημιουργεῖ τὴν ἐπὶ πλέον ἀπαίτησιν ὅπως ἀντέχουν εἰς θερμοκρασίας μεταξὺ 180°C καὶ 205°C κατὰ τὴν περίοδον ὅπου ὑφίστανται στατικὰς καὶ ἐναλλακτικὰς καταπονήσεις εἰς τὰς μεγάλας ταχύτητας πτήσεως τῶν σκαφῶν αὐτῶν. Ἐπιπροσθέτως σύνθετα ὑλικὰ ἐκ πολυμερῶν ὑψηλῆς ἀντοχῆς χρησιμοποιοῦνται ὅλον καὶ περισσότερον εἰς τὰς κατασκευὰς τῶν κινητήρων τῶν ἀεροπλάνων ὅπου εὑρίσκονται ὑπὸ τὴν ἐπίδρασιν θερμοκρασιῶν κυμαινομένων μεταξὺ 370° καὶ 420°C. Κατ' αὐτὸν τὸν τρόπον τὸ ὅριον θερμικῆς εὐσταθείας τῶν ὑλικῶν αὐτῶν ἀνέρχεται εἰς ὑψηλοτέρας θερμοκρασίας καὶ ἑπομένως ἡ ἀντοχὴ τῆς ὀργανικῆς πολυμερικῆς μήτρας τοῦ ὑλικοῦ ἀποτελεῖ τὸ κρίσιμον ὑλικόν. Τοιουτοτρόπως δι' αὐτὰς τὰς περισσότερον δυσμενεῖς συνθήκας λειτουργίας εἰς ὑψηλὰς θερμοκρασίας ὁ χαρακτηρισμὸς τῆς εὐσταθείας τοῦ συνθέτου ὑλικοῦ παρουσιάζεται ὡς ὁ κύριος παράγων ἐρεύνης διὰ τὴν χρησιμοποίησιν τῶν ὑλικῶν αὐτῶν.

Εἰς τὴν ἐργασίαν αὐτὴν μελετᾶται ἡ θερμοοξειδωτικὴ εὐστάθεια σκληρυμένων συνθέτων ὑλικῶν μὲ ἴνας ἀπὸ δισ-μαλαϊμιδικὸν πολυμερὲς καὶ ἄνθρακα μοναξονικοῦ προσανατολισμοῦ δημιουργουμένων διὰ ἐπιθέσεων σειρᾶς διαστρώσεων, τῇ βοηθείᾳ δοκιμῶν ἰσοθερμοκρασιακῆς γηράνσεως. Διὰ τῆς ἀκριβοῦς ἐξετάσεως δοκιμίων διαφόρων μεγεθῶν μὲ ποικίλας ἀνισοτρόπους ἰδιότητας καὶ διὰ μετρήσεως τῆς ἀπωλείας τοῦ βάρους των κατὰ τὰς δοκιμὰς προσδιωρίσθησαν αἱ ταχύτητες ἐκφυλισμοῦ τῶν δοκιμίων αὐτῶν κατὰ τὰς τρεῖς κυρίας διευθύνσεις καθὼς καὶ οἱ διάφοροι μηχανισμοὶ ἐκφυλισμοῦ καθ' ἑκάστην διεύθυνσιν.

Ἐξ ἄλλου, ὑπελογίσθησαν οἱ ἐνεργοὶ συντελεσταὶ διαχύσεως, μετρηθέντες ἐπὶ ἀνεπηρεάστου πυρηνικῆς ζώνης, διὰ τὸν καθορισμὸν τῶν κυρίων διευθύνσεών των καὶ ἐχρησιμοποιήθησαν διὰ τὴν πρόβλεψιν τῶν ταχυτήτων ἐκφυλισμοῦ τοῦ συνθέτου ὑλικοῦ εἰς διάφορα δοκίμια μὲ διαφόρους προσανατολισμοὺς καὶ μεγέθη ἰνῶν. Αἱ κατ' αὐτὸν τὸν τρόπον ἀναπτυχθεῖσαι ἐξισώσεις τῶν προτύπων προβλέπουν ποσοτικῶς τὸ μέγεθος ἀπωλείας τῶν δοκιμίων, ἀποδεικνύοντα τὴν ἰσχὺν τῆς μεθόδου καθορισμοῦ τοῦ ἐκφυλισμοῦ τῶν τρισδιαστάτων ἀνισοτρόπων συνθέτων ὑλικῶν. Τελικῶς, αἱ ζῶναι ἐκφυλισμοῦ παρετηρήθησαν διὰ μικροσκοπίου νὰ κινοῦνται ἐντὸς τῆς ἀνεπηρεάστου πυρηνικῆς ζώνης μὲ τὴν αὔξησιν τοῦ χρόνου γηράνσεως. Ὑπελογίσθη ὅτι ὁ χρόνος γηράνσεως ἐξαρτᾶται σημαντικῶς ἀπὸ τὸν προσανατολισμὸν τῶν ἰνῶν, ὁ ὁποῖος συμβάλλει εἰς τὴν ἀνισοτροπίαν τοῦ συνθέτου ὑλικοῦ. Τόσον ἡ θεωρία, ὅσον καὶ τὰ πειραματικὰ ἀποτελέσματα, ἀπέδειξαν ὅτι ἡ θερμοοξειδωτικὴ εὐστάθεια τῶν συνθέτων ὑλικῶν ἐνισχυμένων μὲ ἴνας ἀποτελεῖ ἰδιότητα τοῦ ὑλικοῦ τανυστικῆς μορφῆς (δηλαδὴ ἐξαρτᾶται ἀπὸ τὸ μέγεθος καὶ τὴν διεύθυνσιν τῆς ἀνισοτροπίας), ἂν καὶ μέχρι σήμερον ἦτο παραδεκτὸν ἐκ παραδόσεως ὅτι τὸ μέγεθος αὐτὸ δύναται νὰ μετρηθῇ μόνον μὲ μετρήσεις ἀπωλείας βάρους βαθμωτοῦ τύπου.